

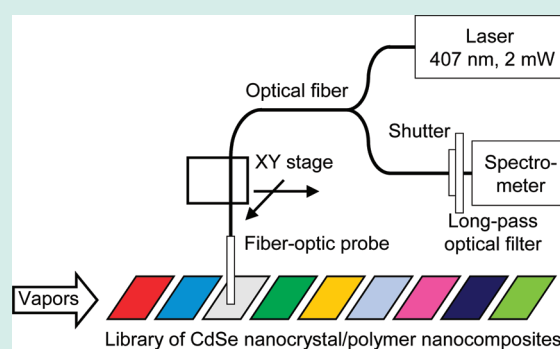
Multisize CdSe Nanocrystal/Polymer Nanocomposites for Selective Vapor Detection Identified from High-Throughput Screening Experimentation

Radislav A. Potyrailo,* Andrew M. Leach, and Cheryl M. Surman

General Electric Company, Global Research Center, Niskayuna, New York 12309, United States

ABSTRACT: We have implemented high-throughput spectroscopic screening tools for the investigation of vapor-selectivity of CdSe semiconductor nanocrystals of different size (2.8- and 5.6-nm diameter) upon their incorporation in a library of rationally selected polymeric matrices. This library of resulting sensing materials was exposed to polar and nonpolar vapors in air. Each of the sensing materials demonstrated its own photoluminescence vapor-response patterns. Two criteria for the evaluation of vapor responses of the library of sensing materials included the diversity and the magnitude of sensing responses. We have found several polymer matrices that simultaneously meet these criteria. Our new sensing materials based on polymer-embedded semiconductor nanocrystal reagents of different size promise to overcome photobleaching and short shelf life limitations of traditional fluorescent organic reagent-based sensing materials.

KEYWORDS: high-throughput screening, spectroscopy, vapor selectivity, CdSe semiconductor nanocrystals, rational design, polymeric matrix, photoluminescence, sensing material



1. INTRODUCTION

Insufficient selectivity of vapor responsive sensing materials¹ is a significant barrier for the practical implementations of individual vapor sensors. While individual sensors with partially selective sensing materials can be arranged in an array,² it was shown that sensor arrays based on partially selective sensing materials fail in the presence of high levels of interferences.³ Further, minimization of the number of sensors in an array simplifies deposition of sensing materials, device fabrication, and data analysis and reduces data processing noise.^{4–6} Thus, development of individual sensors with improved selectivity is an active area of research.

Application of nanomaterials for vapor sensing promises to bring not only enhanced sensitivity^{7,8} and improved response and recovery times⁹ but also improved selectivity.^{10–13} Nevertheless, additional concepts for enhancement of vapor-response selectivity are needed for the implementation with different transducers. Optical transduction methods based on wavelength-multiplexed spectral measurements have a potential to improve the selectivity of vapor responses of individual sensors and sensor arrays. This potential can be realized if individual spectral responses from the sensor or array of sensors are sufficiently independent and are correlated to specific vapors. We recently reported a new concept for selective chemical sensing based on multiple-color CdSe nanocrystals.¹⁴ We incorporated CdSe nanocrystals of different diameters into a poly(methyl methacrylate) (PMMA) film and have found that each size of CdSe nanocrystals in this polymeric nanocomposite unexpectedly demonstrated its own photoluminescence (PL)

response pattern upon exposure to polar and nonpolar vapors in air. Single-size/single-color CdSe quantum dots with different surface modifying groups were also encapsulated into PMMA films^{15–18} and porous anodic aluminum oxide substrates^{19,20} to study their response to organic vapors.

Rational design of sensing and other functional materials based on prior knowledge is attractive because it promises to avoid time-consuming synthesis and testing of numerous materials candidates. However with the increase of complexity of materials, the scientific ability for the rational materials design becomes progressively limited.²¹ As a result of this complexity, combinatorial, and high-throughput experimentation in materials science has been recognized as a new scientific approach to generate new knowledge.^{22–25}

In this study, we have implemented our high-throughput spectroscopic screening tools for the investigation of vapor-sensitivity of CdSe semiconductor nanocrystals of different size upon their incorporation in different polymeric matrices. A library of nine polymeric materials was formulated with 2.8-nm and 5.6-nm diameter CdSe nanocrystals to form multisize CdSe nanocrystal/polymer nanocomposites and was exposed to polar and nonpolar vapors. Two criteria for the evaluation of vapor responses of the library of sensing materials included the diversity and the magnitude of sensing responses. We have found several polymer matrices that simultaneously meet these

Received: July 3, 2011

Revised: December 26, 2011

Published: January 23, 2012

criteria. Our new sensing materials based on polymer-embedded semiconductor nanocrystal reagents of different size promise to overcome photobleaching limitation of traditional fluorescent organic reagent-based sensing materials.

2. EXPERIMENTAL SECTION

2.1. Film Preparation. CdSe nanocrystal solutions in toluene were obtained from Evident Technologies (Troy, NY). Polymers tested as matrices for CdSe nanocrystals were poly(trimethyl-silyl) propyne (Gelest), silicone block polyimide and polycarbonate (General Electric), poly(isobutylene) (Aldrich), poly(methyl methacrylate), polyvinylpyrrolidone, polycaprolactone, poly(dimethylaminoethyl) methacrylate, and styrene-butadiene ABA block copolymer (Scientific Polymer Products). Sensing films were spin-cast from polymer/toluene solutions. The polymer concentration in the solution was 5% vol. The concentrations of 2.8-nm and 5.6-nm diameter CdSe nanocrystals in toluene were the same, 2.5 mg/mL each. The thickness d of these spin-cast films was measured using an interference microscope and was $0.5 \mu\text{m} < d < 1 \mu\text{m}$.

2.2. Measurement Setup and Data Analysis. For high-throughput screening of PL, multiple films with different polymers were arranged as a one-dimensional array. Automatic measurements of PL spectra of the sensing films array were performed using a modular automatic scanning system designed and built in house as detailed earlier.²⁶ Briefly, the system included a 407-nm portable GaN laser (2 mW output power), an in-line optical filter holder, a portable spectrometer, and an X–Y translation stage (see Figure 1). Laser light was

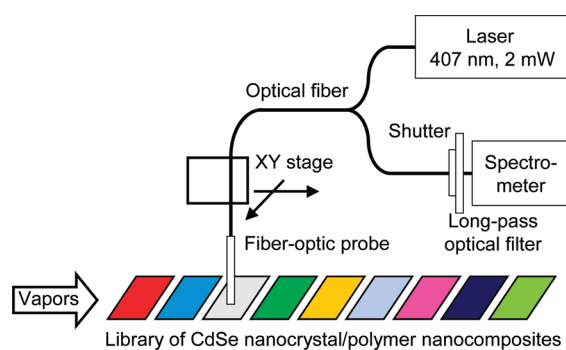


Figure 1. Modular automatic scanning system for high-throughput evaluation of PL spectra of the sensing films array.

focused into one of the arms of a bifurcated fiber-optic reflection probe. The same portable laser was used for photoactivation and PL excitation of sensing films. The uncertainty in measurements of PL intensity using our high-throughput screening system was <2 counts (one standard deviation).

The fabricated sensing films were periodically exposed at room temperature to methanol and toluene vapors at the vapor pressure of 46 and 11 Torr, respectively, using dry nitrogen as a carrier gas. Exposures were done automatically with multiple replicates (at least $n = 3$). Processing of collected spectra was performed using KaleidaGraph (Synergy Software, Reading, PA) and PLS_Toolbox Software operated with Matlab (The Mathworks Inc., Natick, MA). Photoluminescence intensities and spectra were evaluated after subtraction of the dark noise signal of the spectrometer. Principal components analysis (PCA) was done in the range from 450 to 700 nm after mean-centering the data.

3. RESULTS AND DISCUSSION

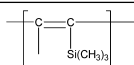
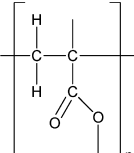
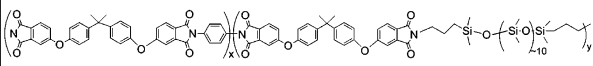
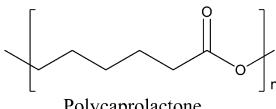
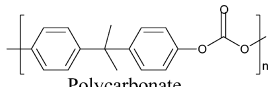
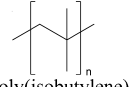
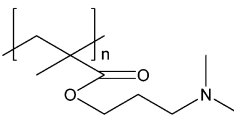
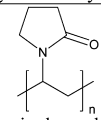
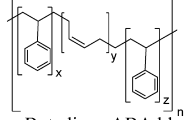
3.1. Rationale for Selection of Polymeric Matrices. To evaluate selectivity of sensing films, we incorporated the analyte-responsive reagents such as CdSe semiconductor nanocrystals of different size into diverse polymeric matrices. A polymer matrix has a tremendous effect on the sensor response in terms of sensor selectivity, sensitivity, and dynamic response.^{25,27} In this study, we have rationally selected several polymeric matrices that have been previously shown to be very effective for vapor sensing.

We included poly(trimethyl-silyl) propyne because it has the largest known solubility of oxygen,²⁸ and thus, it was thought to be a good candidate for efficient vapor-modulated oxidation of CdSe nanocrystals in air. Poly(methyl methacrylate) and polycaprolactone were selected because they are known as efficient matrices for solvatochromic organic dyes²⁹ and, thus, are attractive to be explored with CdSe nanocrystals. Silicone block polyimide was selected because it has very high partition coefficient for sorbing organic vapors³⁰ attractive for its vapor-sensitivity evaluation with CdSe nanocrystals. Poly(dimethylaminoethyl) methacrylate polymer was selected for its surface passivation property of semiconductor nanocrystals.³¹ Polymers with high and low glass transition temperature (T_g), such as polycarbonate and poly(isobutylene), were selected because of their reported diverse vapor-sorption properties^{32,33} and, thus, possibilities for enhanced vapor selectivity. Polyvinylpyrrolidone and styrene-butadiene ABA block copolymer were selected because of their sorption ability of polar and nonpolar vapors, respectively,³⁴ and thus, possibilities for enhanced vapor selectivity. The chemical structures and the rationale for selection of these polymers as a sensing matrix are summarized in Table 1.

3.2. Spectral Properties of Photoactivated Sensing Films. To check for the possibility of interactions between the CdSe nanocrystals of different sizes in toluene solution, we examined PL spectra of the individual sizes of CdSe nanocrystals and their mixture (see Figure 2). The initial PL peak positions of 2.8- and 5.6-nm CdSe nanocrystals in toluene solution were at 541 and 636 nm, respectively. The toluene solution containing the mixture of different nanocrystal sizes exhibited spectral profiles corresponding to the sum of the spectra of the individual sizes of nanocrystals. The lack of spectral distortions or PL peak shifts demonstrated that there were no interactions between the nanocrystals of different sizes. This lack of interactions between the individual nanocrystals is likely because the different size CdSe nanocrystals were passivated with tri-n-octylphosphine oxide (TOPO).^{35,36} Also, the concentration of the nanocrystals in toluene was relatively low leading to only negligible reabsorption affects not affecting the PL intensity ratio.

The 2.8- and 5.6-nm CdSe nanocrystals were further formulated in polymer films and photoactivated with the 407-nm diode laser. Photoactivation is an important aspect of the performance of the CdSe and other semiconductor crystals as chemical sensing materials.¹⁵ Photoactivation has been shown to blue shift nanocrystal emission, attributed to a decrease in size and the photooxidation of the nanocrystal surface.^{37,38} Upon incorporation in polymer films, CdSe nanocrystals exhibited different spectral shifts of PL emission and different emission intensity as illustrated in Figure 3. Upon automatic scanning of fabricated films with the fiber-optic probe with a 1 mm step size, no significant variation on PL intensity was observed across the films.

Table 1. Polymer Matrices for Incorporation of Different Size CdSe Nanocrystals

Sensor #	Polymer structure and name	Rationale for selection as sensor matrix	Ref.
1	 Poly(trimethyl-silyl) propyne	Polymer with largest known solubility of oxygen, candidate for efficient oxidation of CdSe nanocrystals	²⁸
2	 Poly(methyl methacrylate)	Polymer for solvatochromic dyes	²⁹
3	 Silicone block polyimide	Polymer with very high partition coefficient for sorbing organic vapors	³⁰
4	 Polycaprolactone	One of the best polymer matrices for solvatochromic dyes	²⁹
5	 Polycarbonate	Polymer with high T _g for sorbing of organic vapors	³²
6	 Poly(isobutylene)	Polymer with low T _g for sorbing of organic vapors	³³
7	 Poly(dimethylaminoethyl) methacrylate	Polymer for surface passivation of semiconductor nanocrystals that acts as a multidentate ligand	³¹
8	 Polyvinylpyrrolidone	Polymer for sorption of polar vapors	³⁴
9	 Styrene-Butadiene ABA block copolymer	Polymer for sorption of non-polar vapors	³⁴

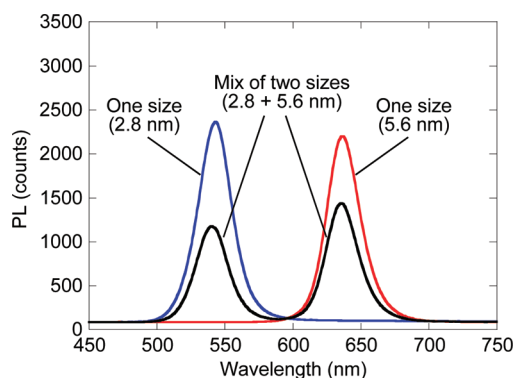


Figure 2. PL spectra of individual size CdSe nanocrystals and their mixture in toluene.

The PL peak positions of 2.8-nm CdSe nanocrystals in the majority of studied polymer nanocomposites were at 501–507 nm and at 514 nm for nanocomposite 1. The PL peak positions of

5.6-nm CdSe nanocrystals in the majority of studied polymer nanocomposites were at 607–620 nm; the PL peak positions were at 580 nm for nanocomposite 4 and at 522 nm for nanocomposite 6 (see Figure 3A). The PL intensity varied from 30 to 297 counts and from 65 to 2868 counts for 2.8- and 5.6-nm CdSe nanocrystals, respectively in different polymers as illustrated in Figure 3B. We believe that the differences in the PL intensity of nanocrystals in different polymers were mostly associated with the photoactivation effects of nanocrystals as evidenced by the different ratio of PL intensities of 2.8- and 5.6-nm CdSe nanocrystals. The film-thickness variation of different polymers contributed to the differences in the PL intensity only to the smaller extent.

3.3. Sensing Response Patterns. Results of exposure of all prepared sensing films to methanol and toluene vapors as the PL changes at their peak positions upon vapor exposures are presented in Figure 4. For consistency and reliability of response of fabricated sensing materials, different films were deposited at the same day over a four-hour time period. To further reduce possible variability, all films were tested using

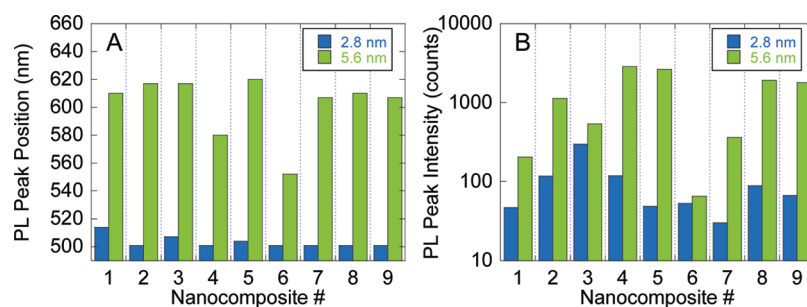


Figure 3. Positions (A) and intensities (B) of PL peaks of CdSe nanocrystals of 2.8- and 5.6-nm embedded in nanocomposite polymer films 1–9 upon photoactivation. Initial PL peak positions of 2.8- and 5.6-nm CdSe nanocrystals in toluene solution were at 541 and 636 nm, respectively.

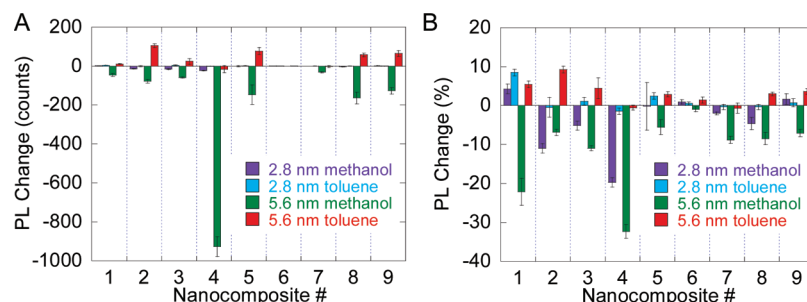


Figure 4. Diversity in steady-state response of the two-size CdSe nanocrystals embedded in nanocomposite polymers 1–9 to polar (methanol) and nonpolar (toluene) vapors: absolute (A) and relative (B) PL response values. Error bars are 1 SD from replicate ($n = 3$) measurements.

the automated testing system as shown in Figure 1. Vapor–response measurements were done in triplicate where Figure 4 presents data with error bars, which are one standard deviation of these replicate measurements. Calculation of standard deviation from this limited number of replicates ($n = 3$) is an accepted practice in chemical analysis.^{39,40} This data indicates a striking diversity in response of the two-size CdSe nanocrystals to these polar and nonpolar vapors. Two aspects of this diversity include the magnitude and direction of the PL change. For example, polymers 2, 4, 5, 8, and 9 show a much larger absolute PL intensity changes as compared to polymers 1, 3, 6, and 7 (see Figure 4A). However, the percent change of PL intensity is largest for polymers 1, 3, and 4 (see Figure 4B).

Polymers employed in this study, were rationally selected according to criteria provided in Table 1. These criteria were based on the previous applications of these polymers in optical sensors with solvatochromic fluorescent dyes and in nonoptical sensors based on gravimetric, resonant, and chemiresistor transducers.^{28–34} On the basis of the results of the present study, it seems that the vapor responses of these polymers when doped with CdSe nanocrystals only slightly follow the expected correlation with earlier reported results for pure polymers and doped with solvatochromic fluorophores. These differences may be attractive to be explored further. In future, these initial experimental results on the effects of toluene and methanol as two initial model vapors (as summarized in Figure 4) should be expanded further to vapors of more diverse nature.

3.4. Response Reversibility and Stability. Reversibility and stability of PL emission of sensing films were tested upon an extended irradiation with the laser light. Such response reversibility and stability are critical in continuous monitoring applications. The key parameters of interest in these evaluations were (1) response of sensing films upon exposures to vapors, (2) recovery of sensing films upon exposures to the carrier gas

(dry nitrogen), (3) the overall stability of the PL intensity, and (4) the stability of the response pattern to methanol and toluene vapors. As an example, Figure 5 shows response patterns from 2.8- and 5.6-nm nanocrystals in polymer 2 film over 16 h of continuous exposure of the film to laser radiation. During the laser exposure, the sensor film was periodically exposed to methanol and toluene vapors. The long-term stability data for this and other polymers indicated that the response of new selective sensor films was very stable upon extended exposure to laser excitation without significant degradation of emission intensity. The response pattern to methanol and toluene was more stable for 5.6 nm nanocrystals as compared to 2.8 nm nanocrystals. This signal stability is a significant advantage of these CdSe nanocrystal/polymer nanocomposite films over films based on organic fluorophores immobilized into polymeric and inorganic films.^{41,42}

3.5. Multivariate Spectral Analysis. The capability for discriminating vapors using a single nanocomposite sensing film with incorporated CdSe nanocrystals of different size was evaluated from individual PL responses of nanocrystals of different size using PCA technique.⁴³ PCA is a commonly used unsupervised and robust pattern recognition approach for analysis of multivariate data. PCA projects the data set onto a subspace of lower dimensionality with removed collinearity. PCA achieves this objective by explaining the variance of the data matrix in terms of the weighted sums of the original variables without significant loss of information. These weighted sums of the original variables are called principal components (PCs). In PCA, the scores plots show the relations between analyzed samples (different vapors in our studies).

The scores plots of the first three PCs are shown in Figure 6, illustrating the diversity of performance of all sensing polymers. The larger the distance between polymer data points, the larger the difference in the response pattern between the respective CdSe/polymer nanocomposites. The first two PCs explained

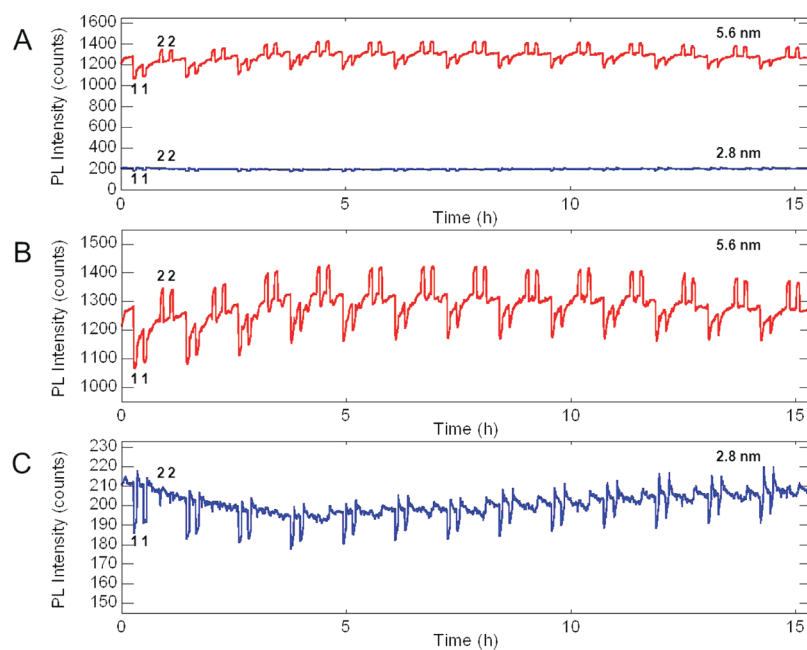


Figure 5. Long-term stability of PL response of polymer 2 film with 2.8- and 5.6-nm CdSe nanocrystals upon repetitive exposures to methanol (1) and toluene (2) vapors: PL intensity from 2.8 and 5.6 nm (A), 5.6 nm (B), and 2.8 nm (C) CdSe nanocrystals.

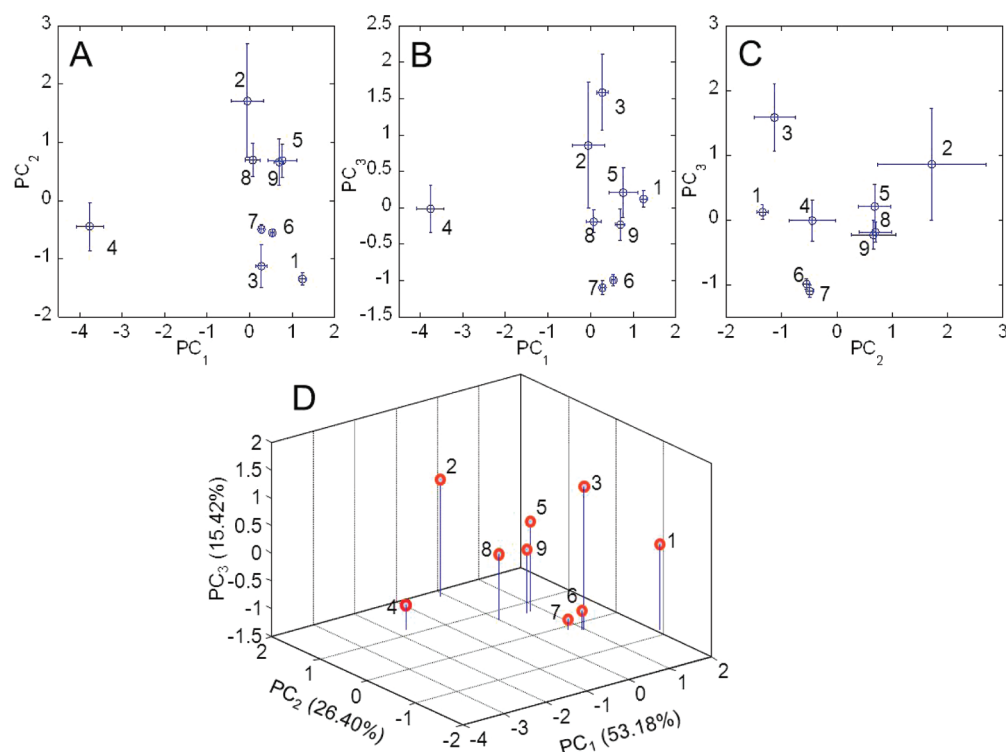


Figure 6. PCA scores plots of the first three principal components of the gas response of nine polymer types with incorporated two-size CdSe nanocrystals: (A) PC_1 vs PC_2 , (B) PC_1 vs PC_3 , (C) PC_2 vs PC_3 , and (D) PC_1 vs PC_2 vs PC_3 . Error bars in (A–C) are 1 SD from replicate ($n = 3$) measurements. Names of polymers 1–9 are provided in Table 1.

only $\sim 80\%$ of the total variation captioned by the PCA model, while the first three PCs explained $\sim 95\%$ of the total variation. Thus, three PCs were used for analysis. An example of such difference is the relatively large distance between polymers 1, 2, and 4 and other polymers as shown on the plot of PC_1 vs PC_2 (see Figure 6A) and PC_1 versus PC_2 versus PC_3 (see Figure 6D). The difference in the response patterns of the multisize CdSe

nanocrystal/polymer nanocomposites could be related to the combined effects of the dielectric medium surrounding the nanocrystals, their size, and oxidation as well as the vapor-sorption characteristics of the polymer.

To quantify this diversity, cluster analysis was further performed where the distances based on principal component scores were adjusted to unit variance. This distance measure,

known as Mahalanobis distance,⁴³ accounts for the different amount of variation in different directions. Results of cluster analysis of PL response patterns upon exposure to methanol and toluene after incorporation into polymeric matrices are demonstrated in the dendrogram in Figure 7 that was

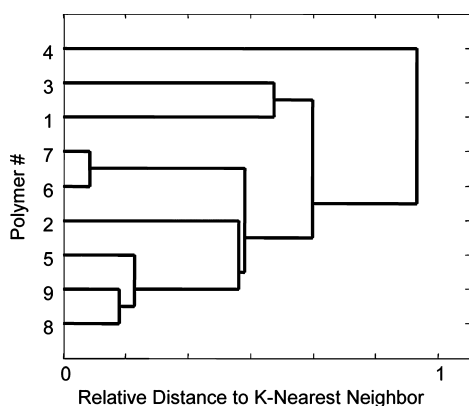


Figure 7. Quantitative analysis of diversity in response to polar and nonpolar vapors of all screened polymers. Dendrogram of cluster analysis using Mahalanobis distance on three PCs of the PCA model. Names of polymers 1–9 are provided in Table 1.

constructed by using Mahalanobis distance on the first three PCs. Polymers 4, 3, and 1 were the most different from the rest of polymers as indicated by the largest diversity distance to K-nearest neighbor.

Data analysis using dendrograms (also known as clustering algorithms) provides means for robust data mining.^{6,44} In this work, such data mining tools provide a means to quantitatively evaluate polymer matrices. When coupled with quantitative structure–property relationships simulation tools that will incorporate molecular descriptors, new knowledge generated from high-throughput experiments may provide additional insights for the rational design of gas sensors based on incorporated semiconductor nanocrystals. In future, such work in vapor sensors promises to complement existing solvatochromic organic dye sensors with more photostable and reliable sensing materials.

Examination of Figures 6 and 7 demonstrates that multisize CdSe nanocrystal/polymer nanocomposites with polymers 1, 2, 3, 4, and 8 have the most diverse spectral responses upon vapor exposures. This diversity is signified by the large distances between these polymers in the scores plots (Figure 6) and in the dendrogram plot (Figure 7). Other polymers, for example polymers 6 and 7, are very close in their response diversity as indicated by the very short distances between these polymers in the scores plots (Figure 6) and in the dendrogram plot (Figure 7).

We explored spectral responses of sensing materials using multivariate tools such as loadings plots of the PCA models of PL spectra over the 450–700 nm spectral range. In PCA, the loadings plots show the relations between analyzed variables (different spectral wavelengths in our studies) and provide the guidance for the selection of the best spectral variables for quantitative analysis.^{45,46} By definition, the spectral loadings are independent from each other and are orthogonal in the loadings plots. Examples of diversity of PL responses of the multisize CdSe nanocrystal/polymer nanocomposites upon exposures to methanol and toluene are presented in Figure 8 for polymers 1, 2, 3, 4, and 8. The first two loadings explained more than 99% of the total variation captioned by the PCA

model, thus only two loadings were used for the detailed spectral analysis. The background of the multivariate spectral analysis that involves the development of PCA models and calculations of respective loadings and the application of loadings for the selection of the best spectral variables for quantitative analysis has been previously reported.^{43,45–47}

The first graph for each polymer (Figure 8A, D, G, J, and M) depicts the mean PL spectrum upon exposures to methanol and toluene and illustrates the relative spectral intensities and peak positions for the two sizes of CdSe nanocrystals in the polymeric matrices. This mean PL spectrum is calculated from the multivariate spectral data analysis of replicate responses to methanol and toluene ($n = 3$) using PCA. As an example, a raw dynamic response is illustrated in Figure 5.

The second graph for each polymer (Figure 8B, E, H, K, and N) depicts the first spectral loading which is the spectrum with the strongest spectral features for the two sizes of CdSe nanocrystals in the polymeric matrices upon exposures to methanol and toluene. Finally, the third graph for each polymer (Figure 8C, F, I, L, and O) depicts the second spectral loading. Analysis of spectral features of polymers depicted in Figure 8 shows the sensitivity and the selectivity of the response of different sizes of the CdSe nanocrystals in different polymeric matrices.

Polymer 1 (Figure 8A, B, and C) possesses a relatively weak (<25% of intensity) and broad spectral PL response of the 2.8-nm nanocrystals compared to the PL intensity of the 5.6-nm CdSe nanocrystals. The contribution to the first loading comes only from the PL spectra of the 5.6-nm CdSe nanocrystals. The contribution to the second loading comes from the PL spectra of both sizes of CdSe nanocrystals with the relatively similar magnitude of spectral contributions.

Polymer 2 (Figure 8D, E, and F) also possesses a relatively weak spectral PL response (<25% of intensity) of the 2.8-nm nanocrystals compared to the PL intensity of the 5.6-nm CdSe nanocrystals. The contribution to the first loading comes mostly from the PL spectra of the 5.6-nm CdSe nanocrystals with only a small contribution from the PL spectra of the 2.8-nm CdSe nanocrystals. The contribution to the second loading comes from the PL spectra of both sizes of CdSe nanocrystals with the relatively strong magnitude of spectral contribution from the 2.8-nm CdSe nanocrystals.

Polymer 3 (Figure 8G, H, and I) possesses an appreciable magnitude (~50% of intensity) of the spectral PL response of the 2.8-nm nanocrystals compared to the PL intensity of the 5.6-nm CdSe nanocrystals. The contribution to the first loading comes mostly from the PL spectra of the 5.6-nm CdSe nanocrystals with only a small contribution from the PL spectra of the 2.8-nm CdSe nanocrystals. However, the contribution to the second loading comes from the PL spectra of both sizes of CdSe nanocrystals with the very strong magnitude of spectral contribution from the 2.8-nm CdSe nanocrystals.

Polymer 4 (Figure 8J, K, and L) possesses a relatively weak (<25% of intensity) and broad spectral PL response of the 2.8-nm nanocrystals compared to the PL intensity of the 5.6-nm CdSe nanocrystals. The contribution to the first loading comes only from the blue-shifted PL spectra of the 5.6-nm CdSe nanocrystals. The contribution to the second loading comes from the PL spectra of both sizes of CdSe nanocrystals with the relatively similar magnitude of spectral contributions.

Polymer 8 (Figure 8M, N, and O) also possesses a relatively weak (<25% of intensity) and broad spectral PL response of the 2.8-nm nanocrystals compared to the PL intensity of the 5.6-nm CdSe nanocrystals. The contribution to the first loading

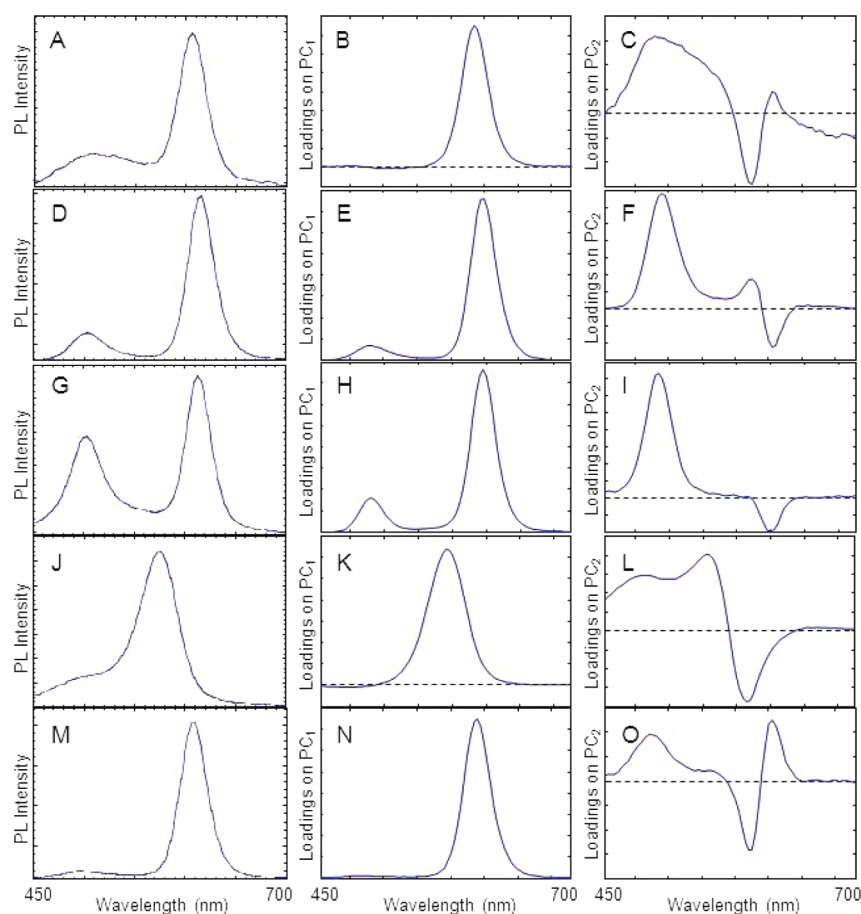


Figure 8. Diversity of PL responses of exemplary multisize CdSe nanocrystal/polymer nanocomposites upon exposures to methanol and toluene shown as the mean PL spectrum upon exposures to vapors (A, D, G, J, and M), the first spectral loading (B, E, H, K, and N), and the second spectral loading (Figure 7C, F, I, L, and O) for each polymer upon exposures to vapors: polymer 1 (A, B, and C); polymer 2 (D, E, and F); polymer 3 (G, H, and I); polymer 4 (J, K, and L); and polymer 8 (M, N, and O).

comes only from the PL spectra of the 5.6-nm CdSe nanocrystals. The contribution to the second loading comes from the PL spectra of both sizes of CdSe nanocrystals with the relatively similar magnitude of spectral contributions.

4. CONCLUSIONS

High-throughput experimentation has been applied for the evaluation of the responses of different-size CdSe nanocrystals incorporated in a variety of rationally selected polymer matrices. Automation of these experiments not only speeds up the screening process of candidate sensing materials, but importantly, reduces or eliminates variation sources that otherwise affect response of the sensing materials if measurements are done manually.

We have found that different polymeric matrices provide diverse response patterns of polymer-incorporated CdSe nanocrystals to vapors of different polarity. Computational studies of the effects of dielectric media on CdSe nanocrystal electronic properties have shown that the absolute value of the dipole moment of the nanocrystal increases with elevated dielectric constant of the surrounding environment.⁴⁸ The magnitude of the change in dipole moment increases with particle size. The elevated diameter and surface area of larger particles means that even small changes in the surface charge of the nanocrystals will result in significant changes in the particles dipole moment. Different size nanocrystals also can have different coverage with the capping TOPO ligand⁴⁹ and when immobilized into a

polymer matrix,³⁶ can contribute to the variable response pattern.

Such work promises to complement existing solvatochromic organic dye sensors with more photostable and reliable sensing materials. Polymers employed in this study, were rationally selected based on their previous applications in optical and nonoptical sensors. However, vapor responses of these polymers when doped with CdSe nanocrystals only slightly follow the expected correlation with earlier reported results for pure polymers and doped with solvatochromic fluorophores. Understanding of these differences may be attractive for future studies. Responses of multisize CdSe nanocrystal/polymer nanocomposites to the broader range of vapors and their concentrations will be also of critical importance in the forthcoming studies.

■ AUTHOR INFORMATION

Corresponding Author

*E-mail: Potyrailo@crd.ge.com.

■ ACKNOWLEDGMENTS

This work has been supported by GE Corporate long-term research funds.

■ REFERENCES

(1) Grate, J. W. Hydrogen-bond acidic polymers for chemical vapor sensing. *Chem. Rev.* **2008**, *108*, 726–745.

- (2) Persaud, K.; Dodd, G. Analysis of discrimination mechanisms in the mammalian olfactory system using a model nose. *Nature* **1982**, *299*, 352–355.
- (3) Peng, G.; Trock, E.; Haick, H. Detecting simulated patterns of lung cancer biomarkers by random network of single-walled carbon nanotubes coated with nonpolymeric organic materials. *Nano Lett.* **2008**, *8*, 3631–3635.
- (4) Röck, F.; Barsan, N.; Weimar, U. Electronic nose: Current status and future trends. *Chem. Rev.* **2008**, *108*, 705–725.
- (5) Joo, S.; Brown, R. B. Chemical sensors with integrated electronics. *Chem. Rev.* **2008**, *108*, 638–651.
- (6) Jurs, P. C.; Bakken, G. A.; McClelland, H. E. Computational methods for the analysis of chemical sensor array data from volatile analytes. *Chem. Rev.* **2000**, *100*, 2649–2678.
- (7) Collins, P. G.; Bradley, K.; Ishigami, M.; Zettl, A. Extreme oxygen sensitivity of electronic properties of carbon nanotubes. *Science* **2000**, *287*, 1801–1804.
- (8) Schedin, F.; Geim, A. K.; Morozov, S. V.; Hill, E. W.; Blake, P.; Katsnelson, M. I.; Novoselov, K. S. Detection of individual gas molecules adsorbed on graphene. *Nat. Mater.* **2007**, *6*, 652–655.
- (9) Snow, E. S.; Perkins, F. K.; Houser, E. J.; Badescu, S. C.; Reinecke, T. L. Chemical detection with a single-walled carbon nanotube capacitor. *Science* **2005**, *307*, 1942–1945.
- (10) Ruminski, A. M.; Moore, M. M.; Sailor, M. J. Humidity-compensating sensor for volatile organic compounds using stacked porous silicon photonic crystals. *Adv. Fun. Mater.* **2008**, *18*, 3418–3426.
- (11) Yang, H.; Jiang, P. Macroporous photonic crystal-based vapor detectors created by doctor blade coating. *Appl. Phys. Lett.* **2011**, *98*, No. 011104.
- (12) Potyrailo, R. A.; Ding, Z.; Butts, M. D.; Genovese, S. E.; Deng, T. Selective Chemical Sensing Using Structurally Colored Core-Shell Colloidal Crystal Films. *IEEE Sensors J.* **2008**, *8*, 815–822.
- (13) Potyrailo, R. A.; Ghiradella, H.; Vertiatchikh, A.; Dovidenko, K.; Cournoyer, J. R.; Olson, E. Morpho butterfly wing scales demonstrate highly selective vapour response. *Nat. Photonics* **2007**, *1*, 123–128.
- (14) Potyrailo, R. A.; Leach, A. M. Selective gas nanosensors with multisize CdSe nanocrystal/polymer composite films and dynamic pattern recognition. *Appl. Phys. Lett.* **2006**, *88*, 134110.
- (15) Nazzal, A. Y.; Qu, L.; Peng, X.; Xiao, M. Photoactivated CdSe nanocrystals as nanosensors for gases. *Nano Lett.* **2003**, *3*, 819–822.
- (16) Vassiltsova, O. V.; Zhao, Z.; Petrukhina, M. A.; Carpenter, M. A. Surface-functionalized CdSe quantum dots for the detection of hydrocarbons. *Sens. Actuators B* **2007**, *123*, 522–529.
- (17) Zhao, Z.; Arrandale, M.; Vassiltsova, O. V.; Petrukhina, M. A.; Carpenter, M. A. Sensing mechanism investigation on semiconductor quantum dot/polymer thin film based hydrocarbon sensor. *Sens. Actuators B* **2009**, *141*, 26–33.
- (18) Knobens, W.; Offermans, P.; Brongersma, S. H.; Crego-Calama, M. Metal-induced fluorescence enhancement as a new detection mechanism for vapor sensing. *Sens. Actuators B* **2010**, *148*, 307–314.
- (19) Amiri, H.; Zhao, Z.; Dansereau, T. M.; Petrukhina, M. A.; Carpenter, M. A. Dependence of hydrocarbon sensitivity on the distance of linked phenyl group to CdSe quantum dots surfaces. *J. Phys. Chem. C* **2010**, *114*, 4272–4278.
- (20) Zhao, Z.; Dansereau, T. M.; Petrukhina, M. A.; Carpenter, M. A. Nanopore-array-dispersed semiconductor quantum dots as nanosensors for gas detection. *Appl. Phys. Lett.* **2010**, *97*, No. 113105.
- (21) Schultz, P. G. Commentary on combinatorial chemistry. *Appl. Catal., A* **2003**, *254*, 3–4.
- (22) Jandeleit, B.; Schaefer, D. J.; Powers, T. S.; Turner, H. W.; Weinberg, W. H. Combinatorial materials science and catalysis. *Angew. Chem., Int. Ed.* **1999**, *38*, 2494–2532.
- (23) Koinuma, H.; Takeuchi, I. Combinatorial solid state chemistry of inorganic materials. *Nat. Mater.* **2004**, *3*, 429–438.
- (24) Rajan, K. Materials informatics. *Mater. Today* **2005**, 38–45.
- (25) Potyrailo, R. A.; Mirsky, V. M. Combinatorial and high-throughput development of sensing materials: The first ten years. *Chem. Rev.* **2008**, *108*, 770–813.
- (26) Potyrailo, R. A.; Olson, D. R.; Medford, G. F.; Brennan, M. J. Development of combinatorial chemistry methods for coatings: High-throughput optimization of curing parameters of coatings libraries. *Anal. Chem.* **2002**, *74*, 5676–5680.
- (27) Potyrailo, R. A. Polymeric sensor materials: toward an alliance of combinatorial and rational design tools? *Angew. Chem., Int. Ed.* **2006**, *45*, 702–723.
- (28) Amao, Y. Probes and polymers for optical sensing of oxygen. *Microchim. Acta* **2003**, *143*, 1–12.
- (29) White, J.; Kauer, J. S.; Dickinson, T. A.; Walt, D. R. Rapid analyte recognition in a device based on optical sensors and the olfactory system. *Anal. Chem.* **1996**, *68*, 2191–2202.
- (30) Potyrailo, R. A.; Sivavec, T. M. Boosting sensitivity of organic vapor detection with silicone block polyimide polymers. *Anal. Chem.* **2004**, *76*, 7023–7027.
- (31) Wang, X.-S.; Dykstra, T. E.; Salvador, M. R.; Manners, I.; Scholes, G. D.; Winnik, M. A. Surface passivation of luminescent colloidal quantum dots with poly(dimethylaminoethyl methacrylate) through a ligand exchange process. *J. Am. Chem. Soc.* **2004**, *126*, 7784–7785.
- (32) Lonergan, M. C.; Severin, E. J.; Doleman, B. J.; Beaver, S. A.; Grubbs, R. H.; Lewis, N. S. Array-based vapor sensing using chemically sensitive, carbon black-polymer resistors. *Chem. Mater.* **1996**, *8*, 2298–2312.
- (33) Ricco, A. J.; Crooks, R. M.; Osbourn, G. C. Surface acoustic wave chemical sensor arrays: new chemically sensitive interfaces combined with novel cluster analysis to detect volatile organic compounds and mixtures. *Acc. Chem. Res.* **1998**, *31*, 289–296.
- (34) Gao, T.; Tillman, E. S.; Lewis, N. S. Detection and classification of volatile organic amines and carboxylic acids using arrays of carbon black-dendrimer composite vapor detectors. *Chem. Mater.* **2005**, *17*, 2904–2911.
- (35) Murray, C. B.; Norris, D. J.; Bawendi, M. G. Synthesis and characterization of nearly monodisperse CdE (E = sulfur, selenium, tellurium) semiconductor nanocrystallites. *J. Am. Chem. Soc.* **1993**, *115*, 8706–8715.
- (36) Kovalevskij, V.; Gulbinas, V.; Piskarskas, A.; Hines, M. A.; Scholes, G. D. Surface passivation in CdSe nanocrystal-polymer films revealed by ultrafast excitation relaxation dynamics. *Phys. Stat. Sol. B* **2004**, *241*, 1986–1993.
- (37) Wang, X.; Qu, L.; Zhang, J.; Peng, X.; Xiao, M. Surface-related emission in highly luminescent CdSe quantum dots. *Nano Lett.* **2003**, *3*, 1103–1106.
- (38) Asami, H.; Abe, Y.; Ohtsu, T.; Kamiya, I.; Hara, M. Surface state analysis of photobrightening in CdSe nanocrystal thin films. *J. Phys. Chem. B* **2003**, *107*, 12566–12568.
- (39) Ingle, J. D., Jr.; Crouch, S. R. *Spectrochemical Analysis*; Prentice Hall: Englewood Cliffs, NJ, 1988.
- (40) *Analytical Chemistry*; Kellner, R., Mermet, J.-M., Otto, M., Widmer, H. M., Ed.; Wiley-VCH: Weinheim, Germany, 1998.
- (41) Wolfbeis, O. S. Materials for fluorescence-based optical chemical sensors. *J. Mater. Chem.* **2005**, *15*, 2657–2669.
- (42) Basabe-Desmonts, L.; Reinhoudt, D. N.; Crego-Calama, M. Design of fluorescent materials for chemical sensing. *Chem. Soc. Rev.* **2007**, *36*, 993–1017.
- (43) Beebe, K. R.; Pell, R. J.; Seasholtz, M. B. *Chemometrics: A Practical Guide*; Wiley: New York, NY, 1998.
- (44) Frenzer, G.; Frantzen, A.; Sanders, D.; Simon, U.; Maier, W. F. Wet chemical synthesis and screening of thick porous oxide films for resistive gas sensing applications. *Sensors* **2006**, *6*, 1568–1586.
- (45) Wise, B. M.; Kowalski, B. R. Process Chemometrics. In *Process Analytical Chemistry*; McLennan, F., Kowalski, B., Eds.; Chapman & Hall: London, England, 1995; pp 259–312.
- (46) Walmsley, A. D. Chemometrics and data treatment. In *Spectroscopy in Process Analysis*; Chalmers, J. M., Ed.; Sheffield Academic Press: Sheffield, England, 2000; pp 336–372.
- (47) Martens, H.; Martens, M. *Multivariate Analysis of Quality. An Introduction*; Wiley: Chichester, England, 2001.

- (48) Rabani, E.; Hetényi, B.; Berne, B. J.; Brus, L. E. Electronic properties of CdSe nanocrystals in the absence and presence of a dielectric medium. *J. Chem. Phys.* **1999**, *110*, 5355–5369.
- (49) Leatherdale, C. A.; Bawendi, M. G. Observation of solvatochromism in CdSe colloidal quantum dots. *Phys. Rev. B* **2001**, *63*, No. (165315)1–6.